Goal Oriented Regional Angular Adaptive Algorithm for the S_N Equations

Bin Zhang*, Liang Zhang, Cong Liu and Yixue Chen

School of Nuclear Science and Engineering, North China Electric Power University, Beijing102206, China
zhangbin@ncepu.edu.cn

Abstract *- Angular discretization errors inherent in the discrete ordinates method are a major problem, especially for localized source problems and problems with strongly absorbing media or large volume of void regions, where angular discretization errors would be totally unacceptable. This paper proposes a regional angular adaptive algorithm together with a goal oriented errors estimate to solve the S_N equations. Standard angular adaptive refinement techniques are based on estimated local errors. We compare an interpolated angular flux value against a calculated value to generate local errors. The adaptive quadrature sets can be created by subdividing a spherical quadrilateral into four spherical sub-quadrilaterals, which have positive weights and can be locally refined. Techniques for mapping angular fluxes from one quadrature set to another are developed to transfer angular fluxes on the interfaces of different spatial regions. To provide a better detector response, local errors are weighted by the importance of a given angular region toward the computational goal, providing an appropriate goal oriented angular adaptivity. First collision source methods are employed to improve adjoint flux calculation accuracy. We tested the performance and accuracy of the proposed goal oriented regional angular adaptive algorithm within the ARES code for a number of benchmark problems, and present the results of one region test model and the Kobayashi benchmark problems. The reduction of angular number is at least one order of magnitude for adaptive refinement. The benchmarks demonstrate that the proposed goal oriented adaptive refinement can achieve the same level of accuracy as the S_N method, which has significantly higher computation cost. Thus, adaptive refinement is a viable approach to investigate difficult particle radiation transport problems.*

Key Words: Discrete ordinates, Goal oriented, Angular adaptive, Ray effects

I. INTRODUCTION

Numerical simulation of multidimensional particle transport processes one of the most difficult problems in applied mathematics. The discrete ordinates method is one of the most widely used techniques to solve the linear Boltzmann equation [1]. However, deterministic solutions of the particle transport equation require discretization of each independent variable, and in some fixed source calculation problems the angular flux may vary greatly in direction. Using low order quadrature sets will result in large errors from ray effects. Due to the inability of low order quadrature sets to accurately compute the required integrals [2], ray effects are unphysical oscillations in the scalar flux and represent the most significant deficiency of the S_N method.

Several methods have been developed to minimize angular discretization errors in discrete ordinates calculations. The simplest approach to mitigate ray effects is to increase the number of discrete directions, but ray effects can persist. Therefore, using higher order quadrature sets to eliminate them is an ineffective strategy [3].

Second class methods use piecewise continuous function expansions to approximate the angular flux. These methods include spherical harmonics (P_N) equivalent fictitious source [4] and angular finite element methods [5]. However, fictitious source iterations seriously affect

convergence rate. To address this difficulty, Miller and Reed [6] proposed a technique where the fictitious source was multiplied by a constant that could take any value between zero and unity. However these methods all suffer from persistent angular discretization errors. The root of the difficulty is that angular flux is far from smooth, and hence not well approximated by piecewise smooth functions that are chosen in advance.

First collision source (FCS) is another method to mitigate ray effects in discrete ordinates calculation [7]. FCS calculates the un-collided flux using a high order transport or analytical method. The un-collided flux generates the first collision source term, which is then applied to calculate the collided flux using the standard S_N method. The total flux distribution is then simply the sum of the un-collided and collided fluxes at each mesh in phase space. Alcouffe [8] modified the standard first collision source method using angle integrated transport balance to define a cell averaged un-collided scalar flux. The accuracy of the un-collided flux calculation is at least of the same order of convergence with mesh refinement as the standard S_N method.

FCS is suitable for solving flux distribution from a spatially localized source in discrete ordinates calculation. However, there are some restrictions, such as volumetric sources problems, where the sources must be approximated using many point sources. Since the un-collided flux is

calculated on a straight line between a source point and target mesh center, the source region must be structured as finite point sources. If the source region is divided too coarsely, the un-collided flux calculation produces large errors. However, when the source region is divided into finer meshes, although error can be reduced, the level of calculation increases proportionally with the number of point sources. In addition, first collision sources generated from these point sources are concentrated in the original source volume, resulting in ray effects from the first collision sources.

Another class of methods to mitigate ray effects is local angular refinement, which adds quadrature points in angular regions where angular flux is highly anisotropic. The regional angular refinement (RAR) technique was developed by Longoni and Haghighat [9,10]. In the RAR method, one or more quadrature points are locally refined into several additional points to provide a large number of quadrature points in one or more directional cones. The RAR technique has been very effective in dealing with highly angular dependent problems [11]. However, the method has a drawback that the directional cones should be selected based on the physical properties of the calculation model.

Recent advances in local angular refinement have focused on adaptive quadrature schemes developed by Stone [12,13] in 2D, and Jarrell [14,15] and Cheuk Y. Lau [16,17] in 3D. These quadrature sets are amenable to local refinement, and hence can be used with an adaptive algorithm. First, the problem is solved on an initial quadrature set, and then a transport sweep is performed to calculate actual values at certain test directions, which are compared with interpolated values at those directions. If the difference between these fluxes exceeds a tolerance, the new quadrature point is added to the quadrature set. These methods are efficient and accurate compared to uniformly refined angles.

Standard angular adaptive refinement techniques are based on locally estimated error, and attempt to equally distributing the error throughout the angular region by refining angles that have large error and coarsening angles with small error. The process continues until the overall error is below a prescribed threshold. However, the angular domain must be split into many small pieces to be solved, and this discretization can consume significant computer memory, which can be a limiting factor.

From a practical engineering point of view, obtaining accurate solutions throughout the entire computational domain may not be necessary. In some shielding problems, where the solution can vary by orders of magnitude over the whole domain, absolute error in low valued regions may be negligible, although the relative error in these regions may be unacceptably high. Thus, the standard angular adaptive method has room for improvement. However, to address the significant computational challenges, goal oriented regional angular adaptive algorithms must be developed. A key step

of goal oriented adaptivity is to solve the adjoint problem to map the importance and estimate the error [18].

Regional angular refinement indicators are composed of both local error and adjoint weight, which describes how important the accuracy of the solution on an angular region is toward the goal of the computation. A regional angular adaptive algorithm together with a goal oriented posteriori error estimate provides the framework for estimating the angular discretization error. This numerical framework was implemented in the neutral particle transport code ARES [19] for assessment.

The remainder of this paper is organized as follows. In Sec. II, we briefly review S_N equations and their variable discretization, and the principles of angle adaptation and derivation of the goal oriented error estimator are discussed. Numerical results for benchmark problems are summarized in Sec. III and we provide concluding remarks in Sec. IV.

II. METHODOLOGY

1. Discrete Ordinates Method

The 3D steady state, single speed linear Boltzmann formulation in Cartesian geometry is

$$\left[\mu_m \frac{\partial}{\partial x} + \eta_m \frac{\partial}{\partial y} + \xi_m \frac{\partial}{\partial z} \right] \psi_m(x,y,z) + \\ \Sigma_t(x,y,z) \psi_m(x,y,z) = Q_m(x,y,z) \tag{1}$$

where

μ_m, η_m, ξ_m = direction cosines for discrete direction Ω_m,

$\psi_m(x,y,z)$ = angular flux at position (x,y,z) and along Ω_m direction within phase-space,

$\Sigma_t(x,y,z)$ = macroscopic total cross section at position (x,y,z),

$Q_m(x,y,z)$ = total source at position (x,y,z) and along Ω_m direction, and

m = angular quadrature index.

Integrating Equation (1) over mesh $(\Delta x_i, \Delta y_j, \Delta z_k)$ and dividing by $\Delta x_i \Delta y_j \Delta z_k$, we obtain the balance equation

$$\frac{\mu_m(\psi_{xout} - \psi_{xin})}{\Delta x} + \frac{\eta_m(\psi_{yout} - \psi_{yin})}{\Delta y} + \\ \frac{\xi_m(\psi_{zout} - \psi_{zin})}{\Delta z} + \Sigma_{t,ijk} \psi_{ijk}^m = Q_{ijk}^m \tag{2}$$

where

ψ_{ijk}^m = average angular flux within mesh space (i,j,k) and along direction Ω_m,

in, out = incoming and outgoing fluxes, respectively,

$\Delta x, \Delta y, \Delta z$ = mesh dimensions along X, Y, and Z axials, respectively,

Q_{ijk}^m = average angular source for mesh (i, j, k) and along Ω_m direction.

The average angular source mesh is

$$Q_{ijk}^m = \sum_{n=0}^{N} \frac{2n+1}{4\pi} \Sigma_{s,ijk}^n \left[\sum_{k=0}^{n} \phi_{n,k,ijk}^e Y_{n,k}^{m,e} + \sum_{k=1}^{n} \phi_{n,k,ijk}^o Y_{n,k}^{m,o} \right] \quad (3)$$
$$+ Q_{fission,ijk}^m + Q_{fixed,ijk}^m$$

where

N = anisotropic scattering order,

$\Sigma_{s,ijk}^n$ = nth order Legendre moment of the scattering cross section for mesh (i, j, k),

$Y_{n,k}^{m,e}$ = nth, kth even order spherical harmonic in Ω_m direction,

$Y_{n,k}^{m,o}$ = nth, kth odd order spherical harmonic in Ω_m direction,

$\phi_{n,k,ijk}^e$ = nth, kth even order flux moment,

$\phi_{n,k,ijk}^o$ = nth, kth odd order flux moment,

$Q_{fission,ijk}^m$ = fission source for mesh (i, j, k) and in Ω_m direction, and

$Q_{fixed,ijk}^m$ = fixed source for mesh (i, j, k) and in Ω_m direction.

The flux moments are

$$\phi_{n,k,ijk}^e = \sum_{m=1}^{M} \psi_{ijk}^m w_m Y_{n,k}^{*m,e} \quad (4)$$

and

$$\phi_{n,k,ijk}^o = \sum_{m=1}^{M} \psi_{ijk}^m w_m Y_{n,k}^{*m,o}, \quad (5)$$

where

w_m = quadrature weight of the Ω_m direction,

$Y_{n,k}^{*m,e}$ = nth, kth associated even order spherical harmonic, and

$Y_{n,k}^{*m,o}$ = nth, kth associated odd order spherical harmonic.

In Equation (2), incoming fluxes are known from upwind mesh calculations or from the boundary conditions. Three auxiliary equations are required to solve the system of equations. In this paper, we employ two differencing schemes: diamond differencing with negative flux set-to-zero fixup (DZ) and theta weighted differencing (TW). Accuracy of the diamond differencing scheme (DD) is second order truncation [20]. The difference equations may yield nonphysical negative angular flux and set-to-zero

fixup is commonly used. However, the fixup causes DD to become nonlinear and depart from second order accuracy. To guarantee a nonnegative exiting flux value with positive sources, the TW scheme is developed.

Many sets have been developed and applied to discrete ordinates transport codes, such as level symmetric (LS) [21], Legendre-Chebyshev (P_NT_N) [22] and quadruple range (QR) [23] quadrature sets. These sets are chosen before the problem is run and remain constant throughout the iteration process. Equations (4) and (5) show that forming these moments require accurate integration of the spherical harmonics. Deviations in the flux moments as a result of discrete ordinates angular quadrature integration may lead to angular discretization errors. Ray effects are caused by inaccurate integration of the angular flux, and are most serious when the angular flux varies significantly as a function of angle.

2. Regional Angular Adaptive Algorithm

Efficiency and accuracy are the key aspects for successful computational methods. To balance these aspects, we develop regional angular adaptive discrete ordinates algorithms. These algorithms add directions where the angular flux is not smooth, and allow different quadrature sets in different spatial regions but a single spatial region has the same quadrature sets for all cells. Flux moments can be accurately integrated by improving the angular refined level. The algorithms require that the quadrature sets can be refined locally, have strictly positive weights, and have a massive number of directions. To ease the mapping process from low to high levels, we need quadrature sets that enable nested refinement.

The method for determining the quadrature's ordinates begins with a cube projection onto the unit sphere to form spherical quadrilaterals [17]. The angular domain is divided into three spherical quadrilaterals on a quadrant of the sphere. One equilateral quadrilateral has four directions. The method used to determine the location of the four points was to place the points at respective sub-quadrilateral centroids. Each quadrilateral was divided into four equilateral sub-quadrilaterals to refine each base quadrature and project them onto the unit sphere to generate refinement angles. The quadrature weight was determined by the surface area of spherical sub-quadrilateral associated with the corresponding point. The level-L quadrature set contains $3 \times 4^{L-1}$ sub-squares per base square, resulting in 3×4^L directions per octant. This refinement process can continue for as many steps as necessary to achieve a given solution accuracy.

Figure 1 shows several uniform refinements, where the spheres represent quadrature points and the color represents the point's weight.
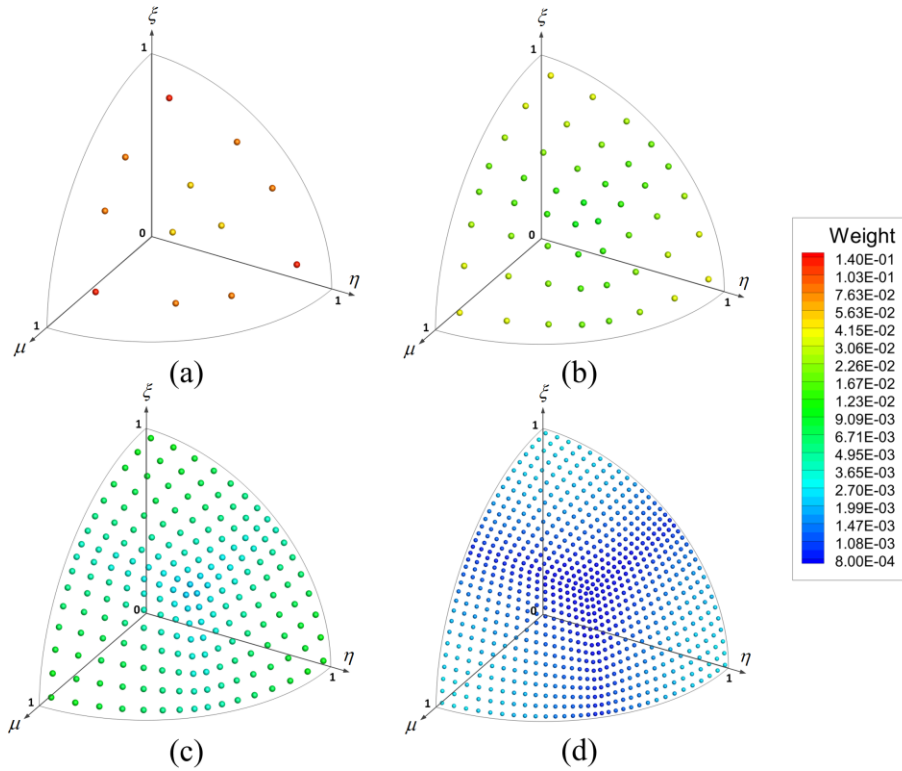
Fig. 1. Uniform refinement of quadrature sets: (a) first, (b) second, (c) third, and (d) fourth level refinements

Figure 2 shows quadrature sets with local regional refinement, incorporating four levels of refinement for the top angular domain, two levels for the left angular domain and three levels for the right angular domain.

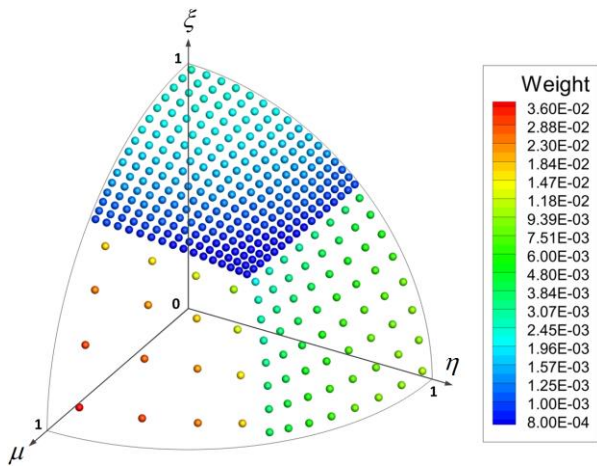Fig. 2. Local regional quadrature sets refinement

Figure 3 shows the flow chart of the adaptive algorithm. The outer is the angle refinement iteration and the inner is the source iteration, where the transport equation is solved. The source iteration is started by updating the source term, and then the angular flux is calculated through a transport sweep. From this angular flux, we update the flux moments and scattering term. For problems with highly scattering regions, the first angular adaptive process is performed after conducting many inner sweeps at the current angular refinement level. In the angular adaptive process, we first calculate the test direction's angular flux, and then generate the angular discretization errors. Quadrature sets are updated if the angular discretization errors are outside a user specified tolerance. We then repeat the process until the error satisfies a convergence criterion.
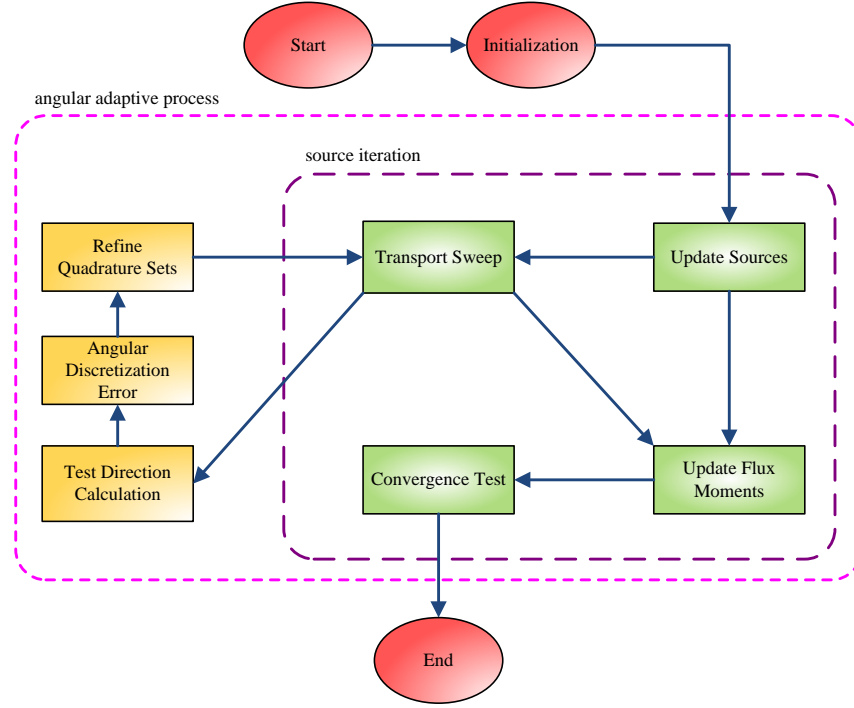
Fig. 3. Schematic flow chart of the regional angular adaptive algorithm

In angular adaptive algorithms, we divide the spatial domain into quadrature regions, which are allowed to have differently refined levels of quadrature sets, but all cells within one quadrature region have the same quadrature sets. The strategy first creates a list of test directions for each region and each octant where the test direction's refinement level is higher than the current refinement level. The test direction can be created with the same level in one octant or one third octant. That is, the whole or part octants have the same angular adaptive level, i.e., regional angular adaptivity. This procedure is repeated region by region and octant by octant.

The angular fluxes at the test directions on all faces of a given region are obtained by a transport sweep using the latest scattering and fixed source as well as the same boundary conditions in the previous transport sweep.

$$\psi_{ijk,calc}^{m'} = \frac{Q_{ijk}^{m'}V_{ijk} + 2|\mu_{m'}|\Delta y\Delta z\psi_{xin} + 2|\eta_{m'}|\Delta x\Delta z\psi_{yin} + 2|\xi_{m'}|\Delta x\Delta y\psi_{zin}}{2|\mu_{m'}|\Delta y\Delta z + 2|\eta_{m'}|\Delta x\Delta z + 2|\xi_{m'}|\Delta x\Delta y + \Sigma_{t,ijk}V_{ijk}}$$

(6)

$$\psi_{xout,calc}^{m'} = 2\psi_{ijk,calc}^{m'} - \psi_{xin}, \qquad (7)$$

$$\psi_{yout,calc}^{m'} = 2\psi_{ijk,calc}^{m'} - \psi_{yin}, \qquad (8)$$

$$\psi_{zout,calc}^{m'} = 2\psi_{ijk,calc}^{m'} - \psi_{zin}, \qquad (9)$$

where

$\psi_{ijk,calc}^{m'}$ = calculated angular flux within mesh space (i,j,k) and along test direction $\Omega_{m'}$,

$\psi_{xout,calc}^{m'}$ = calculated exiting angular flux along each quadrature region boundary at the X direction and along test direction $\Omega_{m'}$,

$\psi_{yout,calc}^{m'}$ = calculated exiting angular flux along each quadrature region boundary at the Y direction and along test direction $\Omega_{m'}$, and

$\psi_{zout,calc}^{m'}$ = calculated exiting angular flux along each quadrature region boundary at the Z direction and along test direction $\Omega_{m'}$.

We then adopt the mapping algorithm to obtain the interpolated angular flux at the test directions along each quadrature region boundary.

Finally, we calculate the difference between the interpolated and calculated angular flux solutions. There are two choices for the difference. The scalar flux difference, $\Delta\phi$, is integration of angular flux over one thirds regions of an octant; and the current difference, ΔJ, is the current along the corresponding perpendicular direction over one thirds regions of an octant.

$$\Delta\phi = \left| \sum_{m'=1}^{M} w_{m'}\psi_{out,calc}^{m'} - \sum_{m'=1}^{M} w_{m'}\psi_{out,interp}^{m'} \right|, \qquad (10)$$

or

$$\Delta J = \left| \sum_{m'=1}^{M} w_{m'} Y_{1,k}^{*m'} \psi_{out,calc}^{m'} - \sum_{m'=1}^{M} w_{m'} Y_{1,k}^{*m'} \psi_{out,interp}^{m'} \right|, \quad (11)$$

where
M = total number of test directions over one thirds regions of an octant;
$\psi_{out,calc}^{m'}$ = calculated exiting angular flux along each quadrature region boundary at the X/Y/Z direction;
$\psi_{out,interp}^{m'}$ = interpolated exiting angular flux along each quadrature region boundary at the X/Y/Z direction; and
$Y_{1,k}^{*m'}$ = associated spherical harmonic, k = 1, 0, -1 corresponding to $\mu_{m'}, \xi_{m'}, \eta_{m'}$.

If the quadrature region's boundary is composed of many cell faces, each cell face should be tested. On any cell face on any boundary of the quadrature region, if the relative differences exceed the desired tolerance, the quadrature sets are refined.

$$\Delta \phi > \varepsilon_{flux} \left| \sum_{m'=1}^{M} w_{m'} \psi_{out,calc}^{m'} \right| \quad (12)$$

or

$$\Delta J > \varepsilon_{current} \left| \sum_{m'=1}^{M} w_{m'} Y_{1,k}^{*m'} \psi_{out,calc}^{m'} \right|, \quad (13)$$

where
ε_{flux} = user-defined scalar flux tolerance and

$\varepsilon_{current}$ = user-defined current tolerance

In angular adaptive algorithms, the mapping schemes are applied to two aspects, the calculation of the interpolated angular flux at the test directions and the transition of angular flux solution between adjacent spatial regions with different quadrature sets during the source iteration process. An optimal mapping scheme should include preservation of both shape and flux moments for incoming angular flux, and resilience against occurrence of negative fluxes. The mapping scheme presented below can be applied to mapping across multiple refinement levels.
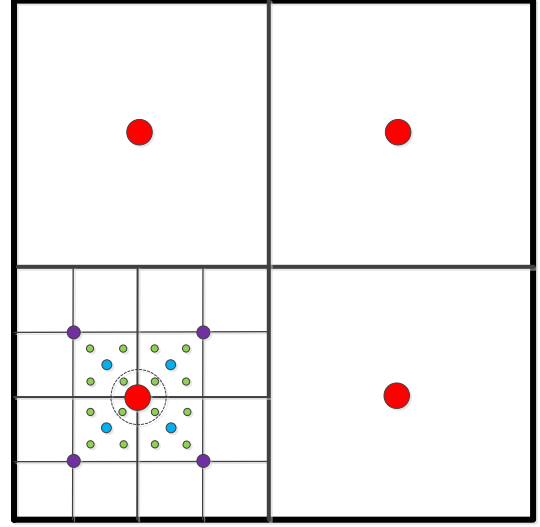

Fig. 4. Fine to coarse mapping

Figure 4 illustrates the fine to coarse mapping scheme that passes angular flux from high level refinement angles to corresponding low level refinement angles. Mapping schemes across multiple refinement levels adopt the same method, where a low order refinement angular flux is calculated using four high order refinement angular fluxes. As shown in Figure 4, mapping across only one refinement level uses four purple points to calculate a red point, mapping across two refinement levels uses four blue points to calculate a red point, and mapping across three refinement levels use four green points in a circle to calculate a red point.

For a direction in low order refinement quadrature sets, we search for the corresponding four sub-directions in high order refinement quadrature sets. The angular flux for this direction can be calculated by a $1/\lambda^l$ weighting scheme, where l is a positive integer and λ represents the shortest distance between this direction and corresponding mapping points on the unit sphere. The angular flux is

$$\psi_{mapped}^{l} = \frac{1}{f^l} \left(\frac{\psi_{fine,1}}{\lambda_1^l} + \frac{\psi_{fine,2}}{\lambda_2^l} + \frac{\psi_{fine,3}}{\lambda_3^l} + \frac{\psi_{fine,4}}{\lambda_4^l} \right), \quad (14)$$

where
$\psi_{fine,1}, \psi_{fine,2}, \psi_{fine,3}, \psi_{fine,4}$ = the known angular fluxes in high order refinement quadrature sets, and
The $l'th$ normalization factor is defined by

$$f^l = \frac{1}{\lambda_1^l} + \frac{1}{\lambda_2^l} + \frac{1}{\lambda_3^l} + \frac{1}{\lambda_4^l}, \quad (15)$$

Following an angular mapping, the zeroth order flux moment or the high order flux moment must be conserved,

$$\psi_{mapped}^{m'} = \frac{\sum_{m=1}^{M_{incoming}} w_m Y_{n,k}^{*m} \psi_{incoming}^m}{\sum_{m'=1}^{M_{mapped}} w_{m'} Y_{n,k}^{*m'} \psi_{mapped}^{m'}} \cdot \psi_{mapped}^{m'}, \qquad (16)$$

where

$\psi_{mapped}^{m'}$ = angular flux for the mapped solution, and

$\psi_{incoming}^m$ = angular flux for the incoming solution.

This mapping scheme ensures conservation of the zeroth order flux moment or the high order flux moment and creates positive flux values at any quadrature points. Due to the adoption of the nearest four point's values, this method also preserves the flux angular shape as far as possible.
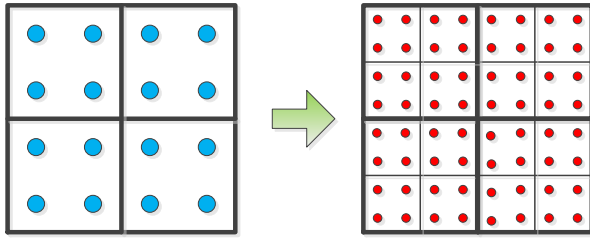

Fig. 5. Coarse to fine mapping

Figure 5 shows the coarse to fine mapping scheme that passes angular flux from low level refinement angles to corresponding high level refinement angles. For coarse to fine mapping, angular flux distribution function over one thirds regions of an octant is fitted by spherical harmonics based on sixteen angular flux values from the incoming solution. The distribution function is

$$\psi(\Omega) = a_0 + a_1\mu + a_2\eta + a_3\xi + a_4 \frac{1}{2}(3\mu^2 - 1) +$$
$$a_5\sqrt{3}\mu\eta + a_6\sqrt{3}\mu\xi + a_7(\sqrt{3}\xi^2 - \frac{\sqrt{3}}{2}(1-\mu^2)) +$$
$$a_8\sqrt{3}\eta\xi + a_9 \frac{1}{2}(5\mu^3 - 3\mu) + a_{10}\frac{\sqrt{6}}{4}\eta(5\mu^2 - 1) + \qquad ,(17)$$
$$a_{11}\frac{\sqrt{6}}{4}\xi(5\mu^2 - 1) + a_{12}(\frac{\sqrt{15}}{2}(\mu - \mu^3) - \sqrt{15}\mu\xi^2) +$$
$$a_{13}\sqrt{15}\mu\eta\xi + a_{14}\sqrt{\frac{5}{8}}(\eta^3 - \eta\xi^2) + a_{15}\sqrt{\frac{5}{8}}(3\eta^2\xi - \xi^3)$$

where

$a_0, a_1, a_2 \cdots a_{15}$ = constants of the polynomial.

The constants are found by solving

$$\begin{bmatrix} 1 & \mu_1 & \eta_1 & \cdots & \sqrt{\frac{5}{8}}(3\eta_1^2\xi_1 - \xi_1^3) \\ 1 & \mu_2 & \eta_2 & \cdots & \sqrt{\frac{5}{8}}(3\eta_2^2\xi_2 - \xi_2^3) \\ 1 & \mu_3 & \eta_3 & \cdots & \sqrt{\frac{5}{8}}(3\eta_3^2\xi_3 - \xi_3^3) \\ \cdots & \cdots & \cdots & \cdots & \cdots \\ 1 & \mu_{16} & \eta_{16} & \cdots & \sqrt{\frac{5}{8}}(3\eta_{16}^2\xi_{16} - \xi_{16}^3) \end{bmatrix} \begin{bmatrix} a_0 \\ a_1 \\ a_2 \\ \cdots \\ a_{15} \end{bmatrix} = \begin{bmatrix} \psi_{coarse,1} \\ \psi_{coarse,2} \\ \psi_{coarse,3} \\ \cdots \\ \psi_{coarse,16} \end{bmatrix},$$
$$(18)$$

where

$\psi_{coarse,1}, \psi_{coarse,2}, \cdots, \psi_{coarse,16}$ = the known angular fluxes in low order refinement quadrature sets.

The mapped angular flux can be obtained from

$$\begin{bmatrix} \psi_{mapped,1} \\ \psi_{mapped,2} \\ \psi_{mapped,3} \\ \cdots \\ \psi_{mapped,64} \end{bmatrix} = \begin{bmatrix} 1 & \mu_1 & \eta_1 & \cdots & \sqrt{\frac{5}{8}}(3\eta_1^2\xi_1 - \xi_1^3) \\ 1 & \mu_2 & \eta_2 & \cdots & \sqrt{\frac{5}{8}}(3\eta_2^2\xi_2 - \xi_2^3) \\ 1 & \mu_3 & \eta_3 & \cdots & \sqrt{\frac{5}{8}}(3\eta_3^2\xi_3 - \xi_3^3) \\ \cdots & \cdots & \cdots & \cdots & \cdots \\ 1 & \mu_{64} & \eta_{64} & \cdots & \sqrt{\frac{5}{8}}(3\eta_{64}^2\xi_{64} - \xi_{64}^3) \end{bmatrix} \begin{bmatrix} a_0 \\ a_1 \\ a_2 \\ \cdots \\ a_{15} \end{bmatrix},$$
$$(19)$$

where

$\psi_{mapped,1}, \psi_{mapped,2}, \cdots, \psi_{mapped,64}$ = the mapped angular fluxes in high order refinement quadrature sets.

The conservation factor is then applied to ensure the zeroth order flux moment or the high order flux moment is preserved using Equation (16). However, this method introduces negative fluxes in some quadrature points, in which case, the nearest point value in low order refinement quadrature sets are used instead of the mapped angular flux.

3. Goal oriented Error Estimate

The adaptive algorithm is a tradeoff between the reduced number of unknowns needed to produce a given accuracy and the overhead of the adaptive error tests. In some shielding transport problems, one is often interested in acquiring an accurate detector response and does not necessarily require an accurate solution across the whole domain. The flux solution may also vary by orders of magnitude from the source region to the region of interest. The absolute error in regions of low values may be

negligible, whereas the relative error in these same regions may still be unacceptably high.

The adaptive algorithm goal is to minimize the error in the detector response with as few as possible unknowns. To achieve this, we need a refinement criterion to choose where refinement in the phase space would be most efficient. The goal oriented adaptive methods provide a better detector response, whereas the traditional adaptive method provides a more accurate global solution. Based on the importance of each particular refinement location for the detector response, we can derive a refinement criterion for the calculation goal. This importance is obtained by solving the adjoint transport equation. The angle is refined when the angular discretization error has a larger contribution to detector response. The monoenergetic adjoint transport equation is

$$-\vec{\Omega}\cdot\nabla\psi^*(\vec{r},\vec{\Omega})+\Sigma_t(\vec{r})\psi^*(\vec{r},\vec{\Omega})=\frac{1}{4\pi}\sigma_D(\vec{r})+$$
$$\sum_{n=0}^{N}\frac{2n+1}{4\pi}\Sigma_s^n(\vec{r})\left[\sum_{k=0}^{n}\phi_{n,k}^{*e}(\vec{r})Y_{n,k}^e(\vec{\Omega})+\sum_{k=1}^{n}\phi_{n,k}^{*o}(\vec{r})Y_{n,k}^o(\vec{\Omega})\right],$$
$$(20)$$

where

$\psi^*(\vec{r},\vec{\Omega})=$ adjoint angular flux,

$\phi_{n,k}^{*e}(\vec{r})=n$th, kth even order adjoint flux moment,

$\phi_{n,k}^{*o}(\vec{r})=n$th, kth odd order adjoint flux moment, and

$\sigma_D(\vec{r})=$ adjoint source.

The differences with the forward transport equation are the sign of the streaming term and a different source term, which is the detector cross section instead of external sources. Solving the adjoint transport equation is actually solving the importance distribution. The larger the adjoint angular flux, the larger the probability that neutrons in that location in phase space will be detected.

An error estimate can be formulated using the forward and adjoint flux. We define the error in the detector response as

$$\Delta J=\left|\sum_{m'=1}^{M}w_{m'}Y_{1,k}^{*m'}\psi_{out,calc}^{m'}-\sum_{m'=1}^{M}w_{m'}Y_{1,k}^{*m'}\psi_{out,interp}^{m'}\right|\cdot\psi_{partial}^*,\ (21)$$

where

$\psi_{partial}^*=$ partial adjoint angular flux,

$$\psi_{partial}^*=\left|\sum_{m=1}^{M}w_m\psi_m^*\pm\sum_{m=1}^{M}w_mY_{1,k}^{*m}\psi_m^*\right|,\qquad(22)$$

The choice of addition and subtraction is determined by the quadrant of the test angle. The local error is weighted by the importance of the computational goal, resulting in appropriate goal oriented error estimates and a fixed percentage of the largest contributions will be refined.

The question that remains is how to calculate the adjoint flux accurately. The solution of adjoint transport equation is almost the same as the forward problem, and can only be solved analytically for a few cases. Therefore, we make some approximations. We can compute the adjoint equation on one refinement level deeper than the forward solution. For simplicity, goal oriented adaptivity often employs the same refinement level for the forward and adjoint problems, and this method captures the essential features even though it is not an exact approximation. We adopt low order quadrature sets or first collision source methods to solve the adjoint equation, and our results show that this simplification is useful.

The first collision source method has been employed to improve calculation accuracy for difficult tasks. The method analytically calculates the un-collided flux to obtain the first collision source term, which is then applied to calculate the collided flux using the standard S_N method. The total flux is composed of the un-collided and collided fluxes. Thus, the first collision source method decomposes the flux into un-collided and collided components

$$\psi^*(\vec{r},\vec{\Omega})=\psi_u^*(\vec{r},\vec{\Omega})+\psi_c^*(\vec{r},\vec{\Omega}),\qquad(23)$$

where

$\psi_u^*(\vec{r},\vec{\Omega})=$ un-collided adjoint flux, and

$\psi_c^*(\vec{r},\vec{\Omega})=$ collided adjoint flux.

The adjoint transport equation is decomposed into

$$-\vec{\Omega}\cdot\nabla\psi_u^*(\vec{r},\vec{\Omega})+\Sigma_t(\vec{r})\psi_u^*(\vec{r},\vec{\Omega})=\frac{1}{4\pi}\sigma_D(\vec{r}),\quad(24)$$

and

$$-\vec{\Omega}\cdot\nabla\psi_c^*(\vec{r},\vec{\Omega})+\Sigma_t(\vec{r})\psi_c^*(\vec{r},\vec{\Omega})=q_{FCS}^*(\vec{r},\vec{\Omega})+$$
$$\sum_{n=0}^{N}\frac{2n+1}{4\pi}\Sigma_s^n(\vec{r})\left[\sum_{k=0}^{n}\phi_{c,n,k}^{*e}(\vec{r})Y_{n,k}^e(\vec{\Omega})+\sum_{k=1}^{n}\phi_{c,n,k}^{*o}(\vec{r})Y_{n,k}^o(\vec{\Omega})\right],$$
$$(25)$$

where

$\phi_{c,n,k}^{*e}=n$th, kth even order collided adjoint flux moment,

$\phi_{c,n,k}^{*o}=n$th, kth odd order collided adjoint flux moment, and

$q_{FCS}^*=$ first collision source terms are calculated from

$$q_{FCS}^*(\vec{r},\vec{\Omega})=$$
$$\sum_{n=0}^{N}\frac{2n+1}{4\pi}\Sigma_s^n(\vec{r})\left[\sum_{k=0}^{n}\phi_{u,n,k}^{*e}(\vec{r})Y_{n,k}^e(\vec{\Omega})+\sum_{k=1}^{n}\phi_{u,n,k}^{*o}(\vec{r})Y_{n,k}^o(\vec{\Omega})\right],$$
$$(26)$$

where

$\phi_{u,n,k}^{*e} = n$th, kth even order un-collided adjoint flux moment, and

$\phi_{u,n,k}^{*o} = n$th, kth odd order un-collided adjoint flux moment.

Although there are some restrictions about how the first collision source method is applied to forward calculation, such as large volumetric sources problem and secondary ray effects, since the computational goal volume is small compared to the whole domain, the method can be applied to the adjoint equation effectively.

III. RESULTS

The goal oriented regional angular adaptive algorithm was implemented in the ARES transport code. ARES is a multi-dimensional parallel discrete ordinates neutral particle transport code that uses state of the art methods to obtain accurate solutions to the Boltzmann transport equation. Preliminary verification and validation for the ARES code system were performed by experiment benchmarking and reference codes. A variety of spatial differencing scheme options are available, including DD with or without linear zero flux fixup, TW, directional theta weighted (DTW); exponential directional weighted (EDW), and linear discontinuous finite element. Traditional source iteration and Krylov iterative method preconditioned with diffusion synthetic acceleration were applied to solve the linear system of equations. ARES uses the Koch-Baker-Alcouffe parallel sweep algorithm to obtain high parallel efficiency.

Algorithm accuracy and efficiency were tested with a few cases from simple to more challenging problems. We first analyzed a fixed source problem with a single quadrature region and ten cells. This allowed testing the adaptive algorithm without impact from mapping schemes. We then expanded to test mapping schemes.

The Kobayashi benchmarks provide significant challenges to the traditional algorithm, with deep penetration, narrow gap, and significant material discontinuity. We were not concerned with computing time at this stage, but rather with whether the proposed algorithm could achieve a given accuracy with significantly fewer unknowns. To examine the algorithm effectiveness, we compared the number of angle unknowns and error norms for all cases using the L_2-norm,

$$L2-norm = \left[\sum_{i=1}^{N} \left(\frac{flux_{calculated}^i - flux_{reference}^i}{flux_{reference}^i} \right)^2 \right]^{1/2} , \quad (27)$$

where
$N =$ the number of solutions at the detector positions,
$flux_{calculated}^i =$ calculated flux at the detector position, and
$flux_{reference}^i =$ reference flux at the detector position.

1. Ten Cells Test Case

To analyze the adaptive algorithm efficiency and accuracy without mapping schemes, a single region test problem containing ten cells with vacuum boundary was adopted. The dimension of each cell was $1 \times 1 \times 1$ cm and a fixed source was located in the first cell. The total cross section was assumed to be 0.1 cm^{-1} with isotropic scattering and scattering ratio = 0.5. The transport calculation utilized DD with linear-zero flux fixup for spatial discretization. We calculated this problem with uniform refined and locally adaptive quadrature sets, LS quadrature sets, and $P_N T_N$ quadrature sets. The reference solution was defined as the scalar flux obtained from level seven refinement uniform quadrature sets with 49152 directions per octant.

Figure 6 shows L_2 error in the cell averaged scalar flux for different octant averaged angular number. In this test problem, the adaptive sets show excellent convergence compared to other quadrature sets. LS quadrature sets, the most widely used, are not suitable for this test case, because of their limitation to order S_{20}. LS quadrature sets are also designed to integrate smooth functions over the global angular domain, and hence poorly integrate functions over local angular regions. Since this case had highly peaked angular flux, results from LS quadrature sets were very inaccurate.

Compared to uniform refinement, the proposed adaptive algorithm can achieve the same accuracy with approximately one-sixth the numbers of quadrature points. In the deterministic transport solver, computation time is approximately proportional to the number of computational cells. The proposed algorithm appears to be a useful tool for high fidelity numerical simulations in neutron transport. In this single quadrature region test case, highly peaked angular flux in the last few meshes, as shown in Figure 7, causes a deep refinement to the quadrature sets.
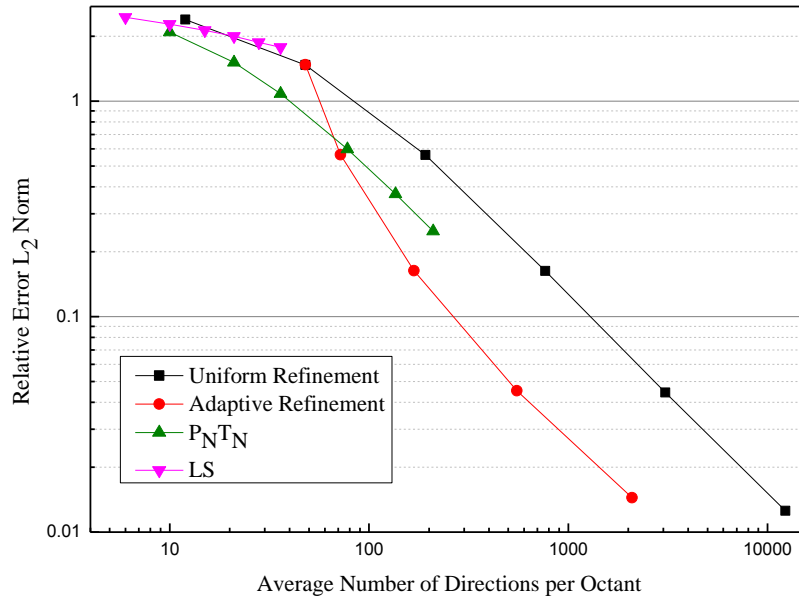
Fig. 6. Scalar flux L_2 error for ten cells test case
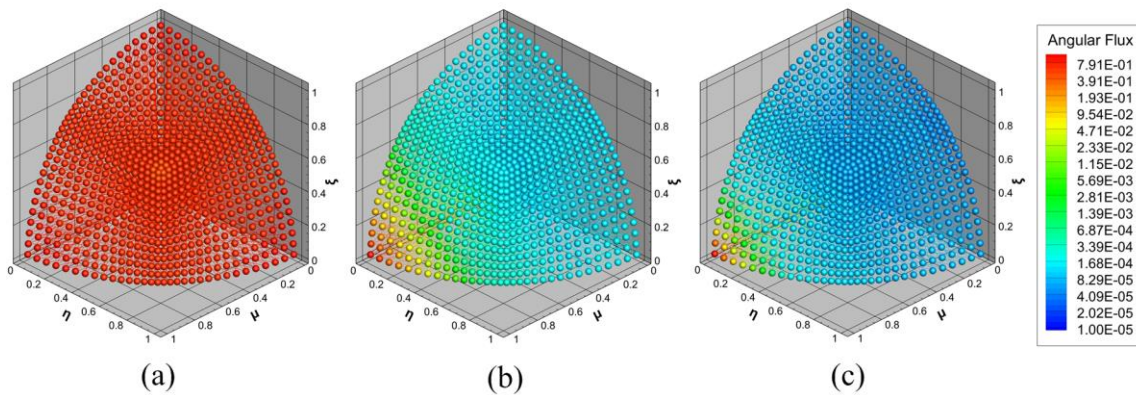

Fig. 7. Angular flux distribution: (a) first mesh, (b) fifth mesh, and (c) last mesh

2. Mapping Method

To demonstrate mapping scheme abilities, a two region test problem containing sixteen cells was adopted. There were 4, 2, and 2 cells along the X, Y, and Z axes, respectively. A uniform isotropic source was placed within the first region. Total cross section was assumed = 0.1 cm^{-1} with isotropic scattering and scattering ratio = 0.5. The left, bottom, and back boundaries were assumed to be reflective, with other boundary conditions to be vacuum. The first region adopted second level refinement quadrature sets and one deeper level was used in the second region.

Figures 8 and Figure 9 show the coarse to fine and fine to coarse mapped solutions at the interface of two adjacent cells, respectively. These mapping schemes ensure conservation of the zeroth or high order flux moment. Figure 8 shows that the coarse to fine mapping scheme can accurately transfer the angular flux solution between adjacent spatial regions with different quadrature sets. Figure 9 show that the proposed method preserves the angular shape of the angular flux as far as possible, due to adoption of the nearest four point's values.
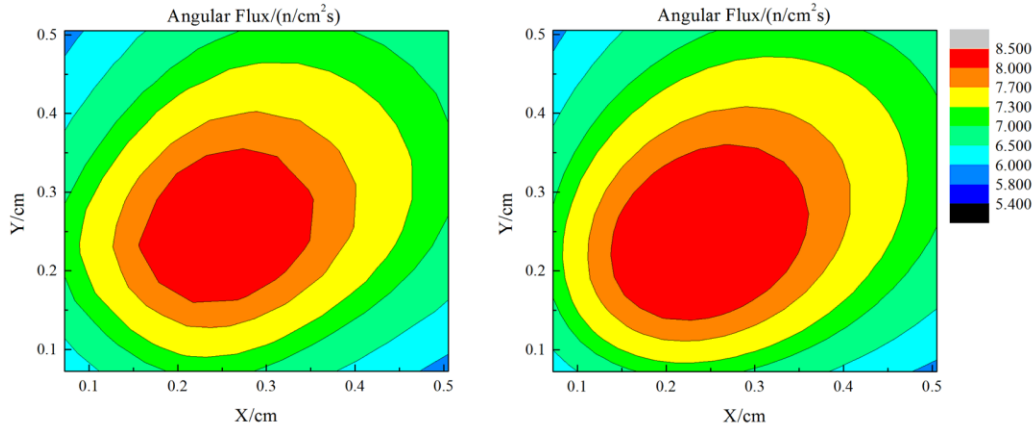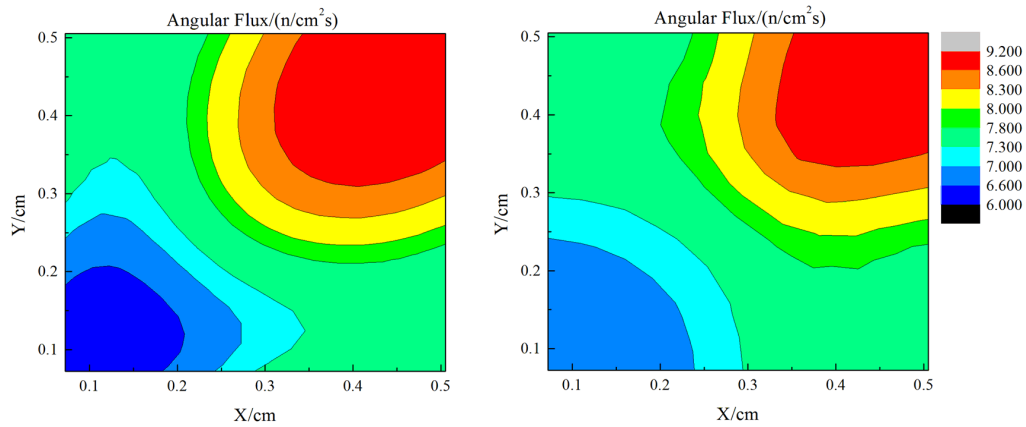
Fig. 8. Angular flux coarse to fine mapped solution

Fig. 9. Angular flux fine to coarse mapped solution

3. Kobayashi Benchmarks

Kobayashi 3D benchmarks with simple geometries and void region were proposed in 1996 to verify the transport codes' solution accuracy [24]. These benchmarks comprise three problems with different geometric models: 1) shield with square void, 2) shield with void duct, and 3) shield with dogleg void duct. Each problem includes case i with no scattering and case ii with 50% scattering. To examine the accuracy and efficiency of the proposed method applying the angular adaptive algorithm with and without goal oriented technique, Kobayashi problems 2 and 3 with 50% scattering medium were calculated and analyzed, as shown in Figures 10 and 11.

The problems were divided into 27 and 64 quadrature regions, respectively, and we adopted 2.0 cm spatial cells using uniform, adaptive, and goal oriented adaptive refinement.
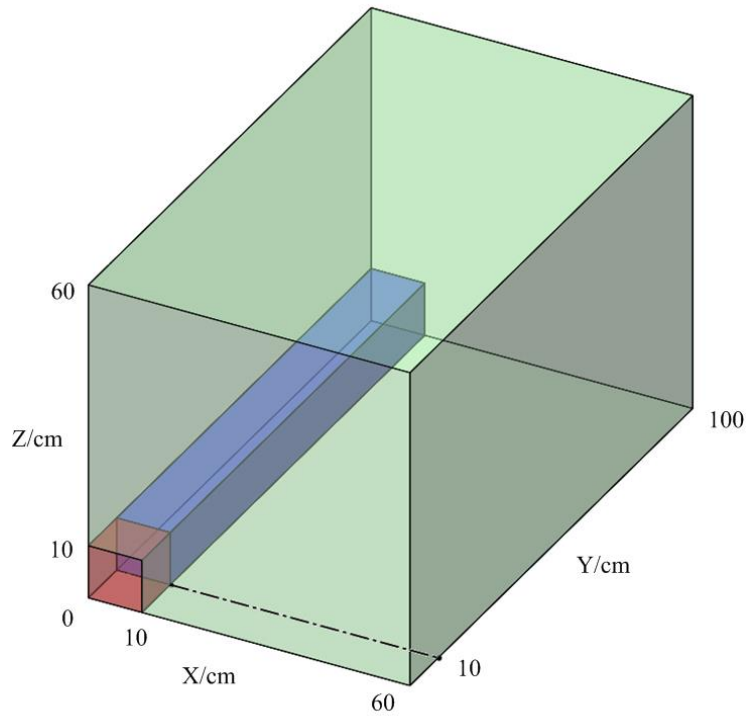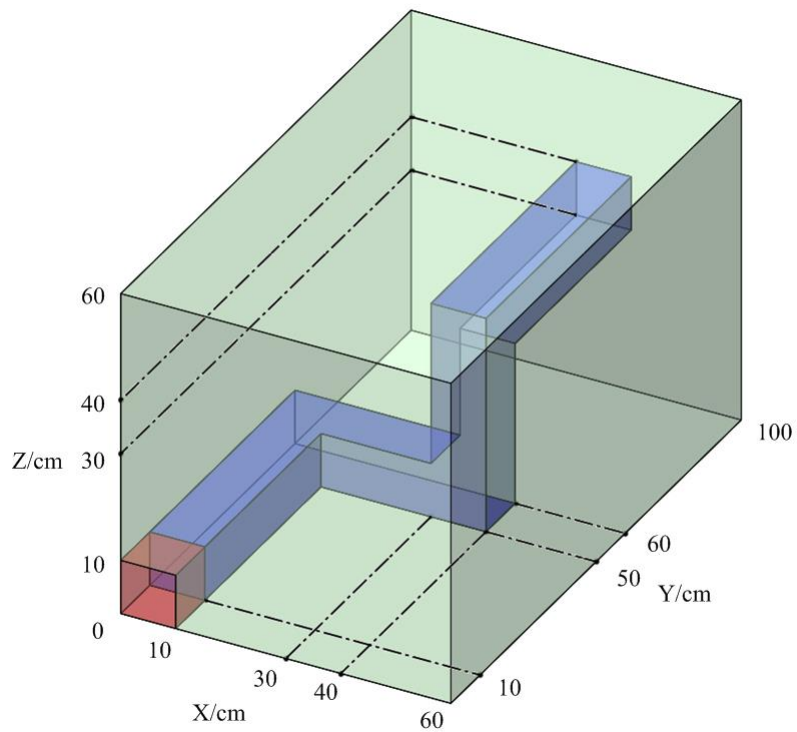
Fig. 10. Kobayashi benchmark problem 2 geometry

Fig. 11. Kobayashi benchmark problem 3 geometry

We present the calculation results of the algorithm and compare with reference solutions [24] for a number of preselected points provided by the benchmark. The reference solutions were used to calculate the scalar flux L_2 error and relative error.

Figure 12 shows cell averaged scalar flux L_2 error as a function of the octant averaged angular number for Kobayashi benchmark problem 2. The proposed goal oriented adaptive refinement shows excellent convergence compared to other refinements. Using the S_N method in the relatively long narrow gap between the source and detector

usually results in serious ray effects. To overcome these effects, the S_N method requires a very large number of quadrature points. L_2 error is large using uniform refinement, while more than 500 octant averaged angular numbers used. The reduction of angular number is at least one order of magnitude for adaptive refinement. When $L_2 < 0.04$, goal oriented adaptive refinement uses approximately 1/60 fewer angles than uniform refinement. Scalar flux error oscillates with adaptive refinement, due to the accuracy of the mapping schemes.
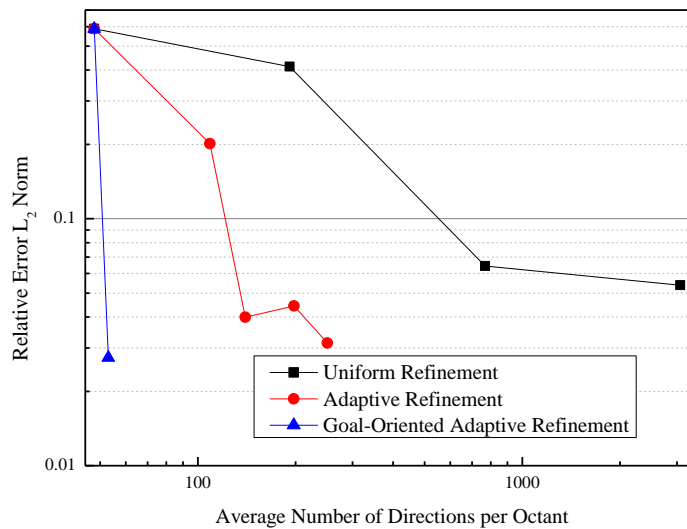

Fig. 12. Scalar flux L_2 error for Kobayashi benchmark problem 2

Figures 13 and 14 show scalar flux L_2 error and the relative error, respectively, as a function of the octant-averaged angular number for Kobayashi benchmark problem 3. Problem 3 is the most difficult Kobayashi problem, since particles tend to stream along the dogleg void duct. This model presents significant challenges to quadrature sets. After every five source iterations, the angular flux solution was tested at each quadrature region boundary to determine if any angular regions needed to be refined. Figure 13 shows the reduction of angular number is more than one order of magnitude for the proposed goal oriented adaptive refinement. The proposed method utilizes adjoint flux of the computational goal, combined with angular adaptivity, to accurately and rapidly compute quantities of interest. Some oscillation is also caused by the

accuracy of mapping scheme, hence a more advanced mapping scheme should be developed.

Figure 14 shows the relative scalar flux error at the duct outlet in the spatial cell centered at (35, 95, 35 cm). The proposed algorithm achieves the same precision with approximately 1/10 fewer unknowns. The goal oriented adaptive refinement is more efficient than uniform refinement because it can generate angles tailored toward a particular goal rather than resolving the solution everywhere.

These benchmarks demonstrate that the proposed goal oriented adaptive refinement can achieve the same level of accuracy as the S_N method with significantly fewer computation cost. Utilization of high quadrature orders is not practical for large problems. Thus, the optimum use of computational resources by means of adaptive refinement is an effective method to analyze difficult particle radiation transport problems.
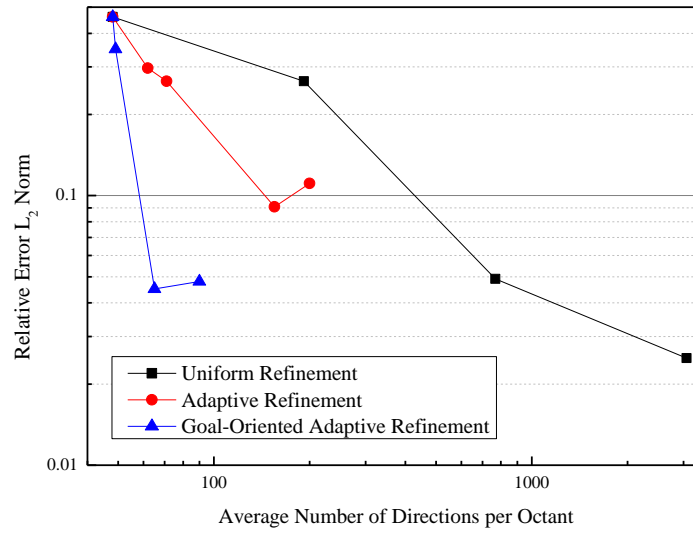
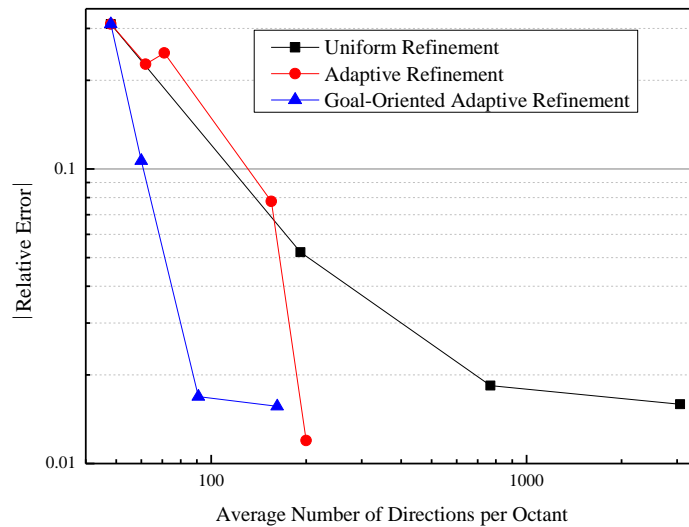Fig. 13. Scalar flux L2 error for Kobayashi benchmark problem 3

Fig. 14. Scalar flux relative error at the duct outlet for the Kobayashi benchmark problem 3.

IV. CONCLUSIONS

We propose a goal oriented regional angular adaptive algorithm to solve the S_N equation, specifically for application to problems containing void regions and narrow gaps. The main goal of the proposed algorithm is to obtain a given accuracy for much lower computational cost than can be obtained with fixed quadrature sets. Forward and adjoint fluxes generate an error estimator, optimize angular discretization, and minimize error in the target engineering output.

Performance and accuracy of the proposed algorithm was tested for a few difficult problems where the traditional S_N method becomes inefficient. The proposed algorithm achieved accurate solutions with significantly reduced number of quadrature points. For the single region test

problem, the adaptive algorithm achieved the same accuracy with approximately 1/6 the number of quadrature points comparing to uniform refinement. For the mapping scheme test problem, the proposed method accurately transferred the angular flux solution and preserved angular flux shape as much as possible. The algorithm was very efficient for the Kobayashi problems, achieving the same accuracy with approximately 1.5 orders of magnitude fewer unknowns than uniform refinement.

The proposed method was tested for a large variety of problems, and the current study provides important proof of concept that the goal oriented error estimation technique is an effective method to analyze difficult shielding transport cases.

We also discussed limitations of the mapping algorithm for passing angular flux between two spatial regions with different quadrature sets. The next major challenge is to investigate the effects of coupled spatial and angular resolutions and how spatial discretization affects angular adaptivity. A number of improvements will lead to more practical application of the proposed methodology, such as parallel implementation and angular multigrid acceleration methods.

ACKNOWLEDGMENTS

REFERENCES

1. E. E. LEWIS and W. F. MILLER JR., *Computational Methods of Neutron Transport*, John Wiley & Sons, New York (1984).
2. K. D. LATHROP, "Ray Effects in Discrete Ordinates Equations," *Nucl. Sci. Eng.*, 32, 357 (1968).
3. K. D. LATHROP, "Remedies for Ray Effects," *Nucl. Sci. Eng.*, 45, 225 (1971).
4. J. JUNG, H. CHIJIWA, K. KOBAYASHI, and H. NISHIHARA, "Discrete Ordinates Neutron Transport Equation Equivalent to P_L Approximation," *Nucl. Sci. Eng.*, 49, 1 (1972).
5. L. L. BRIGGS, W. F. MILLER, JR., and E. E. LEWIS, "Ray-Effect Mitigation in Discrete Ordinate-Like Angular Finite Element Approximations in Neutron Transport," *Nucl. Sci. Eng.*, 57, 205 (1975).
6. W. F. MILLER, JR. and WM. H. REED, "Ray-Effect Mitigation Methods for Two-Dimensional Neutron Transport Theory," *Nucl. Sci. Eng.*, 62, 391 (1977).
7. R. E. ALCOUFFE, "A First Collision Source Method for Coupling Monte Carlo and Discrete Ordinates for Localized Source Problems," *Joint Los Alamos/CEA Monte Carlo Conference*, France, 1985 (1985).

8. R. E. ALCOUFFE, R. D. O'Dell, and F. W. Brinkley, Jr., "A First-Collision Source Method That Satisfies Discrete Sn Transport Balance," *Nucl. Sci. Eng.*, 105, 198 (1990)
9. G. LONGONI AND A. HAGHIGHAT, "Development of New Quadrature Sets with the 'Ordinate Splitting' Technique," *Proc. of the 2001 ANS International Meeting on Mathematical Methods for Nuclear Applications (M&C)*, Salt Lake City, Utah, USA, September 2001, American Nuclear Society (2001).
10. G. LONGONI and A. HAGHIGHAT, "Development and Application of the Regional Angular Refinement Technique and its Application to Non-conventional Problems," *Proc. PHYSOR 2002*, Seoul, Korea, October 7–10, 2002 (2002).
11. G. LONGONI, *Advanced Quadrature Sets, Acceleration and Preconditioning Techniques for the Discrete Ordinates Method in Parallel Computing Environment*, PhD Thesis, University of Florida (2004).
12. J. C. STONE and M. L. ADAMS, "Progress on Adaptive Discrete-Ordinates Algorithms and Strategies," *Proc. Conf. Nuclear Mathematical and Computational Sciences (M&C2003),* Gatlinburg, Tennessee, April 6-10, 2003, American Nuclear Society (2003).
13. J. C. STONE, *Adaptive Discrete-Ordinates Algorithms and Strategies*, PhD Thesis, Texas A&M University (2007).
14. J. J. JARRELL, *An Adaptive Angular Discretization Method for Neutral-Particle Transport in Three-Dimensional Geometries*, PhD Thesis, Texas A&M University (2010).
15. J. J. JARRELL and M. L. ADAMS, "Discrete-Ordinates Quadrature Sets Based on Linear Discontinuous Finite Elements," *Proc. Int. Conf. Mathematics and Computational Methods Applied to Nuclear Science and Engineering (M&C 2011)*, Rio de Janeiro, Brazil, May 8-12, 2011, American Nuclear Society (2011).
16. C. Y. LAU and M. L. ADAMS, "Discrete-ordinates Quadratures Based on Linear and Quadratic Discontinuous Finite Elements Over Spherical Quadrilaterals," *Proc. of the 2015 ANS Joint International Conference on Mathematics and Computation (M&C 2015)*, LaGrange Park, IL April 19–23, 2015, American Nuclear Society (2015).
17. C. Y. LAU, *Adaptive Discrete-Ordinates Quadratures based on Discontinuous Finite Elements over Spherical Quadrilaterals*, PhD Thesis, Texas A&M University (2016).
18. B. TURCKSIN, J. C. RAGUSA, and W. BANGERTH, "Goal-Oriented h-Adaptivity for the Multigroup SPN Equations," *Nucl. Sci. Eng.*, 165, 305 (2010).
19. L. ZHANG, B. ZHANG, P. ZHANG, M. CHEN, J. ZHAO, S. ZHANG, and Y. CHEN, "Verification of ARES Transport Code System with TAKEDA Benchmarks," *Nucl. Instrum. Methods Phys. Res. Sect. A Accel. Spectrom. Detect. Assoc. Equip.*, 797, 297 (2015).

20. E. W. LARSEN, "Spatial Convergence Properties of the Diamond Difference Method in x, y Geometry," *Nucl. Sci. Eng.*, 80, 710 (1982).

21. K. D. LATHROP and B. G. CARLSON, "Discrete Ordinates Angular Quadrature of the Neutron Transport Equation," LA-3186, Los Alamos Scientific Lab. (1964).

22. W. F. WALTERS, "Use of the Chebychev-Legendre Quadrature Set in Discrete-Ordinates Codes," *Proc. Conf. Numerical Methods in High-Temperature Physics*, LA-11342-C, Los Alamos National Laboratory (1988).

23. I. K. ABU-SHUMAYS, "Angular Quadratures for Improved Transport Computations," *Transp. Theory Stat. Phys.*, 30, 169 (2013).

24. K. KOBAYASHI, N. SUGIMURA, and Y. NAGAYA, "3D Radiation Transport Benchmark Problems and Results for Simple Geometries with Void Region," *Prog. Nucl. Energy*, 39, 119 (2001).